THE UNIVERSITY OF MICHIGAN

COLLEGE OF ENGINEERING
Department of Electrical Engineering
Space Physics Research Laboratory

Scientific Report

IONOSPHERIC ELECTRON DENSITY AND BODY POTENTIAL MEASUREMENTS BY A CYLINDRICAL PROBE

Andrew F. Nagy
Ahmed Z. Faruqi

ORA Project 05671

under contract with:

NATIONAL AERONAUTICS AND SPACE ADMINISTRATION
CONTRACT NO. NASr-54(04)
WASHINGTON, D. C.

administered through:

OFFICE OF RESEARCH ADMINISTRATION ANN ARBOR

September 1964

TABLE OF CONTENTS

LIST OF FIGURES

INTRODUCTION

The first direct ionospheric electron temperature measurements were made by equal area, bipolar Langmuir probes, called "Dumbbells" (Spencer et al., 1962; Brace et al., 1963). The temperatures which were measured by these probes were considerably higher than the accepted values at that time, making these results highly controversial. An equal area bipolar probe, due to its inherent operation, samples only the relatively high energy ambient particles and therefore a non-Maxwellian distribution could result in an erroneous temperature interpretation. To check for this posibility, each of the last two Dumbbell experiments NASA 6.04 and NASA 6.05 carried a cylindrical probe which was operated as a highly unequal area, bipolar Langmuir probe with the whole Dumbbell surface acting as the reference body. This arrangement resulted in a sufficiently high area ratio to permit the sampling of the main portion of the energy distribution. These cylindrical probe experiments indicated that the electron energy distribution is, at least predominantly, Maxwellian in the E and F regions of the ionosphere and that the high temperatures are correct.

The Dumbbell experiments also provided—besides the electron temperature data—ion density information, which was derived from the ion current measurements. The interpretation of the ion current in terms of ambient density is complicated by the following two important effects. The extension of the classical stationary Langmuir probe theory (Mott-Smith and Langmuir, 1926) to satellite or rocket-borne probes, has shown that the ion current is highly

velocity and orientation dependent, since the typical rocket velocities are in the order of the ion thermal velocities. The other effect which complicates the interpretation of the ion current is the photocurrent caused by solar electromagnetic radiation. This photocurrent density is of the order of the random ion current density at about 800 km.

The electron current is relatively insensitive to both of these effects since (a) the electron thermal velocities greatly exceed typical rocket velocities, and (b) the random electron current density is many times greater than the photocurrent density up to several thousands of kilometers. It becomes, therefore, attractive to use the electron current characteristics for the determination of the ambient charged particle density.

In this report three data reduction techniques are used to obtain the electron density and the reference body potential from the experimental electron current characteristics of a cylindrical probe carried by Dumbbell NASA 6.05, which was fired at 23.25 p.m. local time on December 21, 1961, from Wallops Island, Virginia. In the last section the results obtained by the different methods are compared and critically discussed.

THE CYLINDRICAL PROBE EXPERIMENT

A block diagram of the cylindrical probe arrangement used on NASA 6.05 is shown in Fig. 1. The collector was 7 in. long with a diameter of .022 in. The 3 in. coaxial guard electrode, which was maintained at the same potential as that of the collector, ensured that the collecting cylinder was outside the sheath of the Dumbbell and it also helped in maintaining a uniform sheath at the inner collector termination. The current to this guard was not measured as indicated in the block diagram shown in Fig. 1. During the "cylindrical probe" mode of operation, a 3 c/s sawtooth voltage was applied to the collector and the guard, with the entire Dumbbell surface acting as the reference.

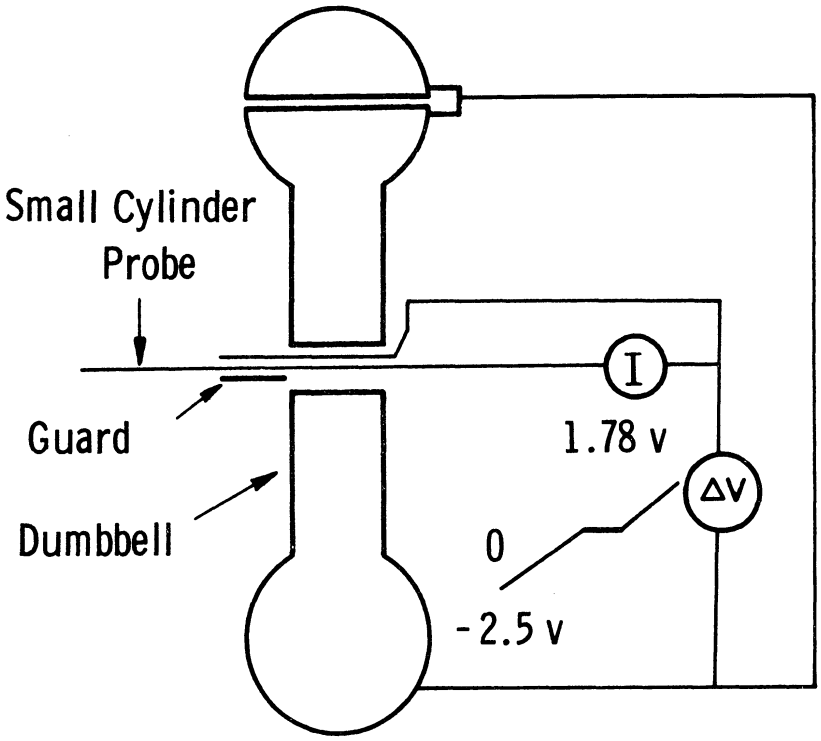

Fig. 1. Block diagram of cylindrical probe system.

THEORETICAL BACKGROUND

The equations for the current collected by a stationary cylindrical probe immersed in a plasma, were derived by Mott-Smith and Langmuir (1926). An extension of this work to moving cylindrical probes was carried out recently by Kanal (1964). In obtaining his equations Kanal assumed a coaxial cylindrical sheath about the moving probe, which can only be considered as a first-order approximation, but which is used until a better model is obtained. The resulting general equations for the retarded and accelerated currents respectively, are:

$$I_r = \left(\frac{kT}{2m\pi}\right)^{1/2} NqA \exp\left(-V_o-\kappa^2\right) \sum_{n=o}^{\infty} \frac{(2n+1)!\ \kappa^n}{(n!)^2\ 2^{2n} V_o^{n/2}}\ I_n\left(2\kappa V_o^{1/2}\right) \qquad (1)$$

$$I_a = \left(\frac{kT}{2m\pi}\right)^{1/2} NqA\ \frac{2}{\pi^{1/2}} \exp\left(-\kappa^2\right) \sum_{n=o}^{\infty} \frac{\kappa^n}{n!} \left[\exp\left(V_o\right)\cdot V_o^{-n/2}\ \Gamma\left(n+\frac{3}{2},\ V_o\left(1+\gamma_o^2\right)\right)\right.$$

$$\left. \times J_n\left(2\kappa V_o^{1/2}\right) + \frac{a}{r}\frac{\kappa^n}{n!}\ \gamma\left(n+\frac{3}{2},\ \gamma_o^2 V_o\right)\right]$$

where:

k = Boltzmann's constant

T = temperature

m = mass

N = number density

q = electronic charge

A = collector area

$\kappa = \lambda \sin \Theta$

$\lambda = W/C_a$

W = magnitude of the probe velocity

C_a = most probable speed of the particle under consideration

$= (\frac{2kT}{m})^{1/2}$

θ = angle between the probe velocity vector and the probe axis

$V_o = \frac{qV_{pp}}{kT}$

V_{pp}= potential difference between the probe and the ambient plasma

$= V_{ap} + V_D$

V_{ap}= applied voltage

V_D = potential of the Dumbbell with respect to the plasma

$I_n(x)$ = modified Bessel function of the first kind and order n

$\gamma_o = (\frac{r^2}{a^2 - r^2})^{1/2}$

r = probe radius

a = sheath radius

$\Gamma(v,x)$= incomplete gamma function

$= \int_x^\infty \exp[-t]\, t^{v-1}\, dt = \Gamma(v) - \gamma(v,x)$

$\gamma(v,x) = \int_0^x \exp[-t]\, t^{v-1}\, dt$

$J_n(x)$= Bessel function of order n

Since the thermal velocity of the electrons is very large in comparison with typical spacecraft velocities, κ can be considered to be zero for electrons. The Debye length corresponding to typical nighttime F-region conditions is of the order

of 1 cm. The dimension of the sheath which surrounds the collector is of the order of the Debye length and since the radius of the collector used in this experiment is only .027 cm, a very large a/r ratio (sheath radius to probe radius) results. The current Eqs. (1) and (2) for $\kappa \to 0$ and $a/r \to \infty$ are given by Eqs. (3) and (4), respectively

$$I_r \Big|_{\kappa \to 0} = \left(\frac{kT}{2m\pi}\right)^{\frac{1}{2}} NqA \exp(-V_o) \tag{3}$$

$$I_a \Big|_{\substack{\kappa \to 0 \\ \frac{a}{r} \to \infty}} = \left(\frac{kT}{2m\pi}\right)^{\frac{1}{2}} NqA \left[\frac{2}{\pi^{1/2}} V_o^{1/2} + \exp(V_o)\, \mathrm{erfc}\,(V_o^{\frac{1}{2}})\right] \tag{4}$$

where:

$$\mathrm{erfc}\,(x) = \text{complimentary error function}$$

$$= 1 - \frac{2}{\pi^{1/2}} \int_o^x \exp[-\beta^2]\, d\beta$$

The conditions used to obtain Eqs. (3) and (4) are applicable to the electron current characteristics of a small cylindrical probe of the type used in this experiment. These equations are therefore used for the electron current analysis described in this report. Figures 2 and 3 show the predicted volt-ampere characteristics of the cylindrical probe for a typical set of parameters. These characteristics were plotted using Eqs. (3) and (4) for the electron current and the limit of Eqs. (1) and (2) as $a/r \to \infty$, for the ion current component. Figures 2 and 3 show clearly that the ion current is significantly altered by orientation changes with respect to the velocity vector, while the electron current is essentially independent of this orientation. The curves plotted in these figures assume that the cylinder is not in the wake of any object and the volt-

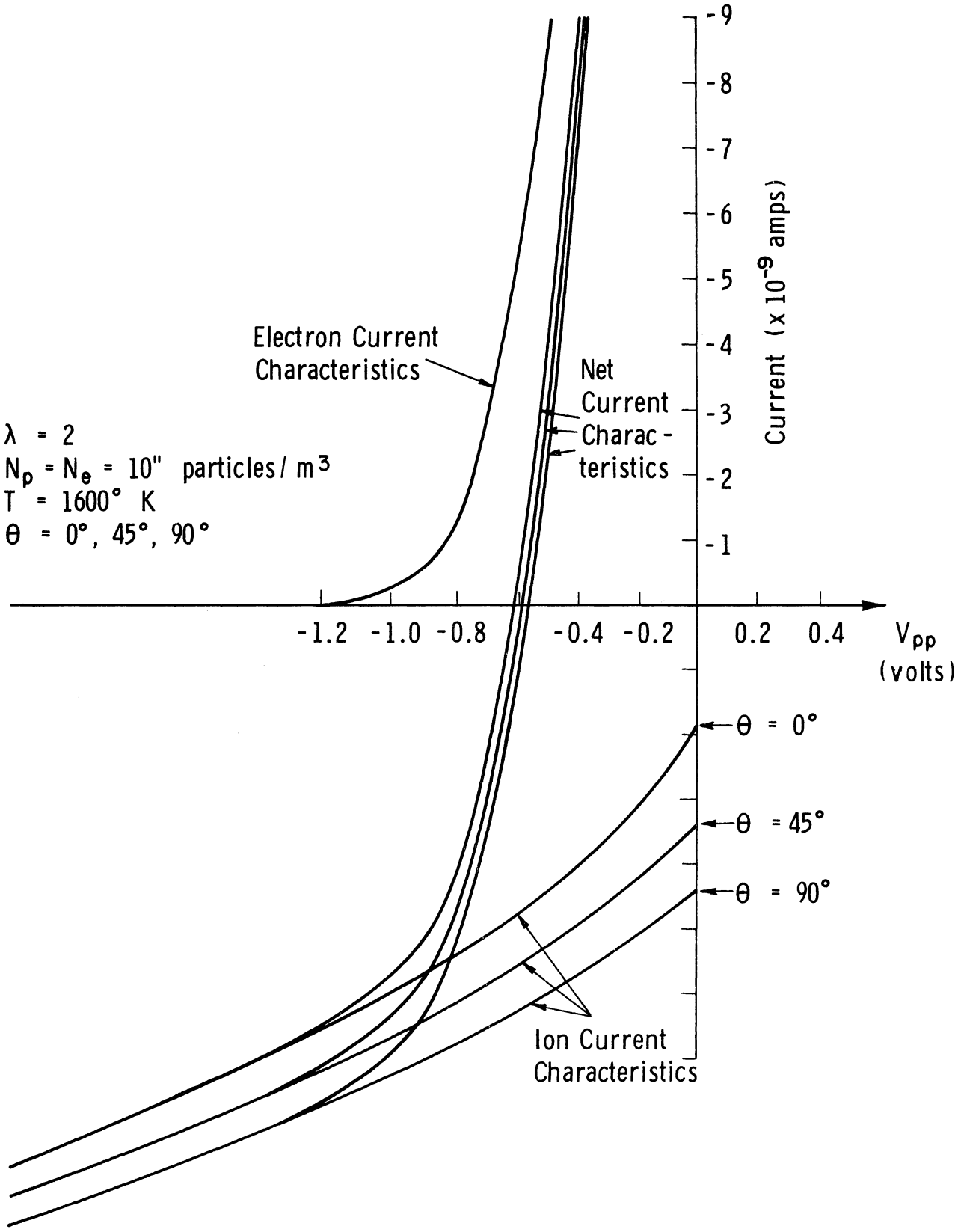

Fig. 2. Theoretical volt-ampere characteristic of a moving cylindrical probe under typical F-region conditions, showing the effect of probe orientation upon the ion current characteristic.

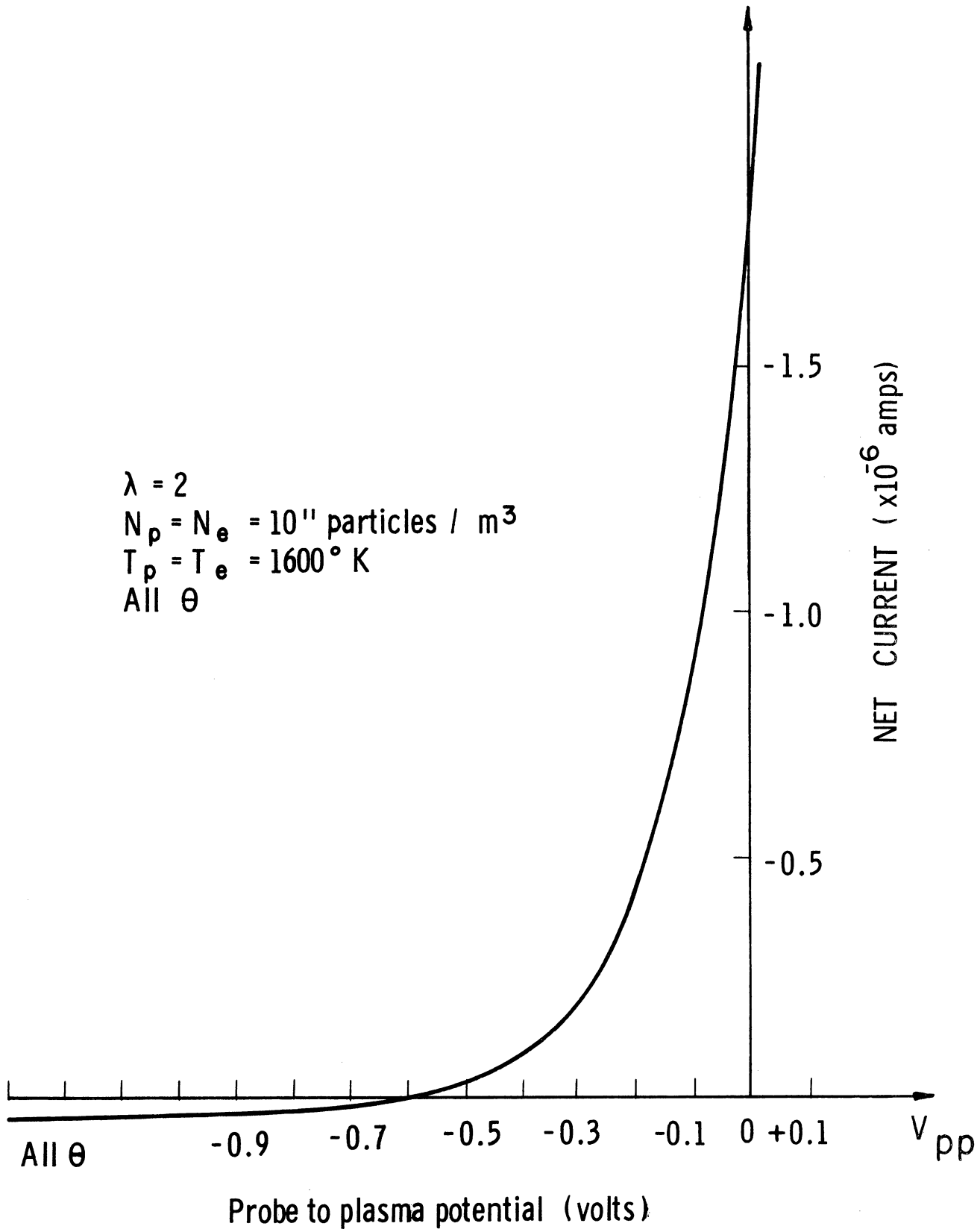

Fig. 3. Theoretical volt-ampere characteristic of a moving cylindrical probe under typical F-region conditions, showing primarily the electron current region of the curve.

ampere characteristics which are analyzed in this report were chosen to satisfy this condition. A typical experimental volt-ampere curve is shown in Fig. 4.

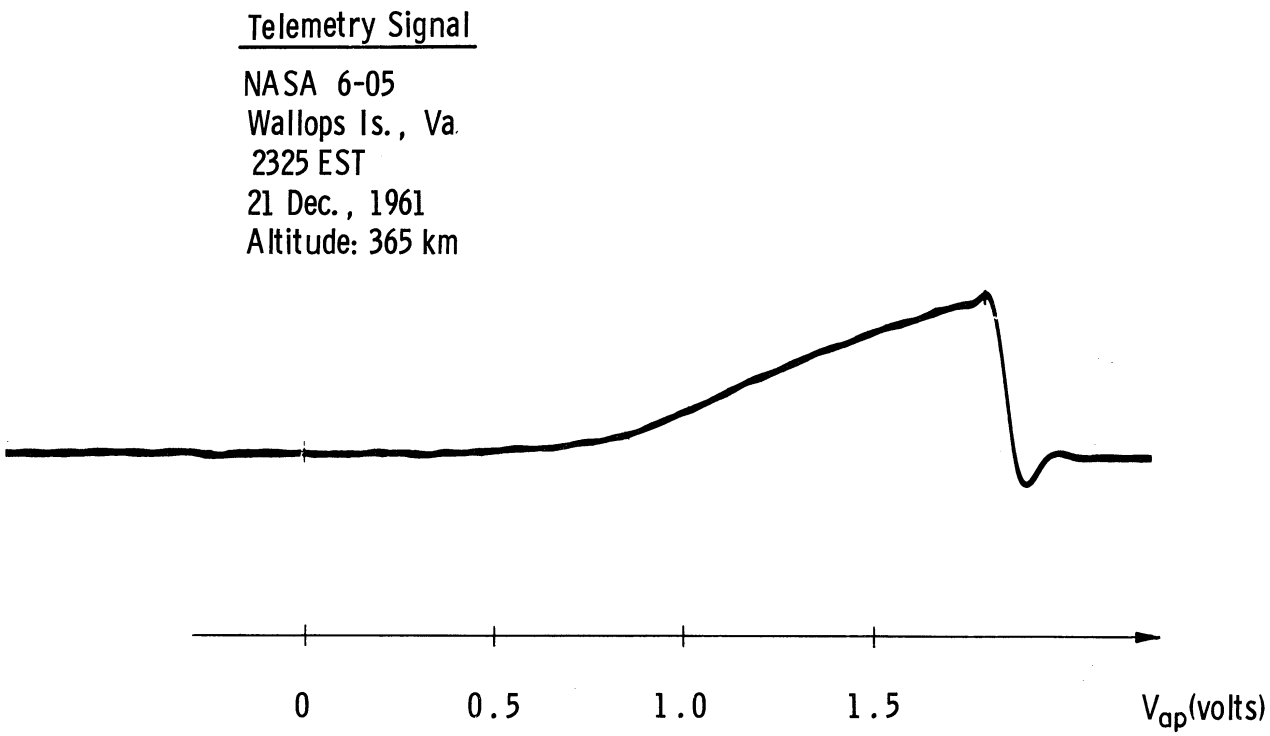

Fig. 4. Typical telemetry data from the cylindrical probe.

VARIOUS DATA REDUCTION METHODS

Equations (3) and (4) indicate that the net potential between the plasma and the probe must be known to permit the determination of the electron density from the electron current. Since the probe is driven against the Dumbbell, the equilibrium potential of the Dumbbell must also be found. The area ratio of the cylindrical collector and guard to the total Dumbbell surface is 350:1. Such a large area ratio is sufficient to assure that the Dumbbell potential stays nearly constant (there is actually a small change which is discussed later) during one sweep of the sawtooth voltage, which is applied to the cylindrical probe. For a constant Dumbbell potential, it is also necessary that the parameters which determine the equilibrium potential such as velocity, orientation, density, temperature, etc., do not change during a sweep period. The 3 c/s voltage function is sufficiently fast with respect to the probe motion to permit this assumption.

The retarded current equation (Eq. 3) shows an exponential relation between the collected current and the voltage, whereas the equation for accelerated current shows a strong departure from such behavior. Therefore, ideally the plot of the electron current as a function of the applied voltage on a semilog paper will result in a straight line for positive applied voltages, up to the point where the cylinder reaches the plasma potential. The applied potential corresponding to this breakpoint is then equal in magnitude and opposite in sign to the equilibrium reference (Dumbbell) potential. Such a curve, constructed from typical experimental points is shown in Fig. 5. A plot of the reference potential, V_D, obtained

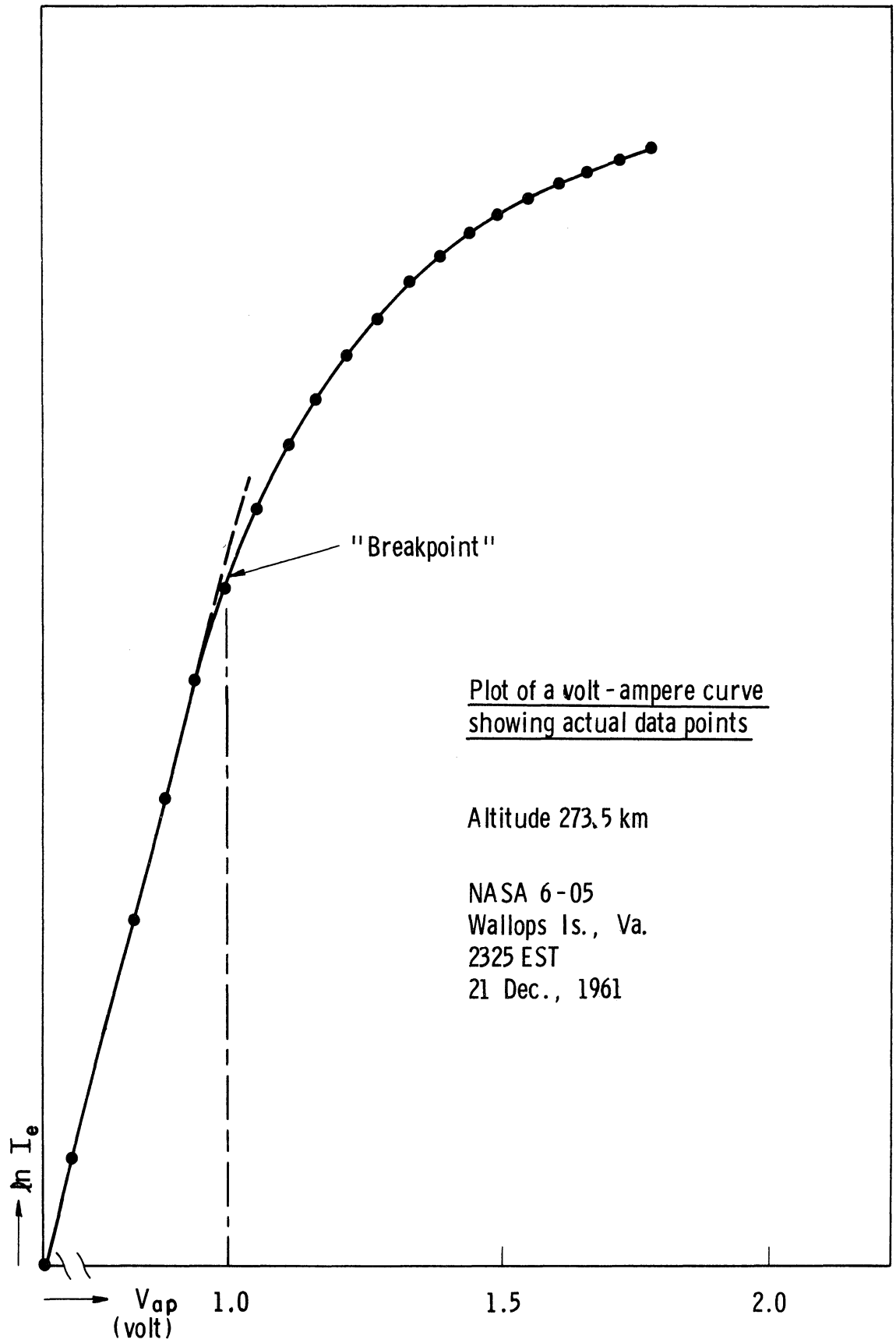

Fig. 5. Plot of a volt-ampere curve showing actual data points.

by this "breakpoint method" (Method I) as a function of altitude is shown in Figs. 6 and 7.

The electron current collected by a probe at the plasma potential, referred to as the random current, is given by Eq. (5).

$$I_{er} = \left(\frac{k\ Te}{2\pi m_e}\right)^{1/2} N_e\ q\ A \qquad (5)$$

where:

T_e = electron temperature

m_e = mass of an electron

N_e = ambient electron density

Once the plasma potential is determined by the breakpoint method, the value of the random electron current can easily be found. Using the electron temperatures derived from the Dumbbell characteristics, the ambient electron densities were calculated from the random electron current. The results of these calculations are plotted on Fig. 8.

Equation (4) for the accelerated current contains two unknowns: the ambient electron density and the reference potential. The fact that these unknowns and the other parameters in Eq. (4) can be considered constant during one sweep, as discussed above, leads to another technique (Method II) for the determination of the electron density and the Dumbbell potential. The method employed is simple; by noting the collected current for two different applied voltage values (selected to ensure accelerating conditions), two equations with two unknowns are obtained, which then are solved. A computer program was written to obtain such solutions

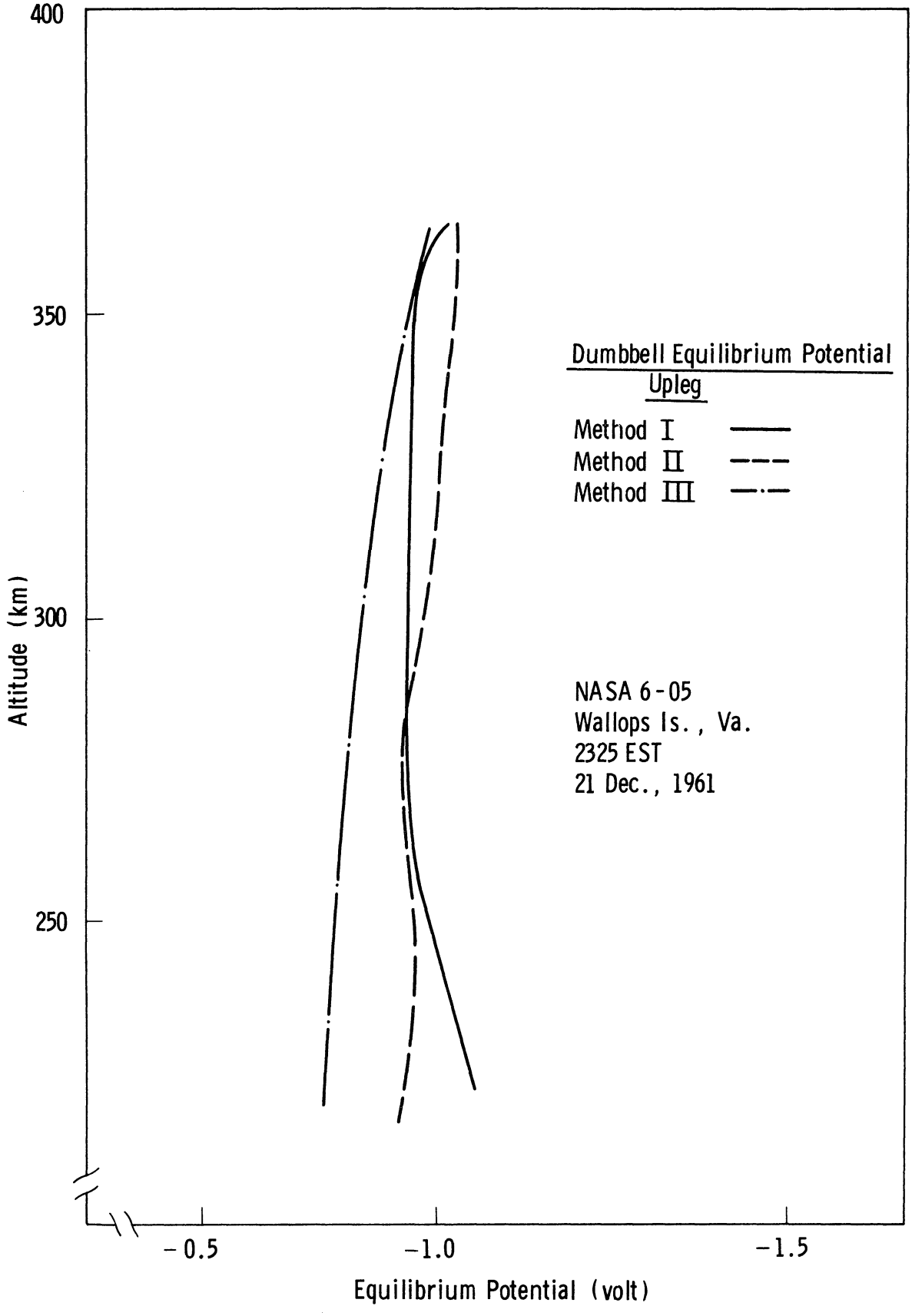

Fig. 6. Upleg Dumbbell equilibrium potential profiles obtained by the three methods.

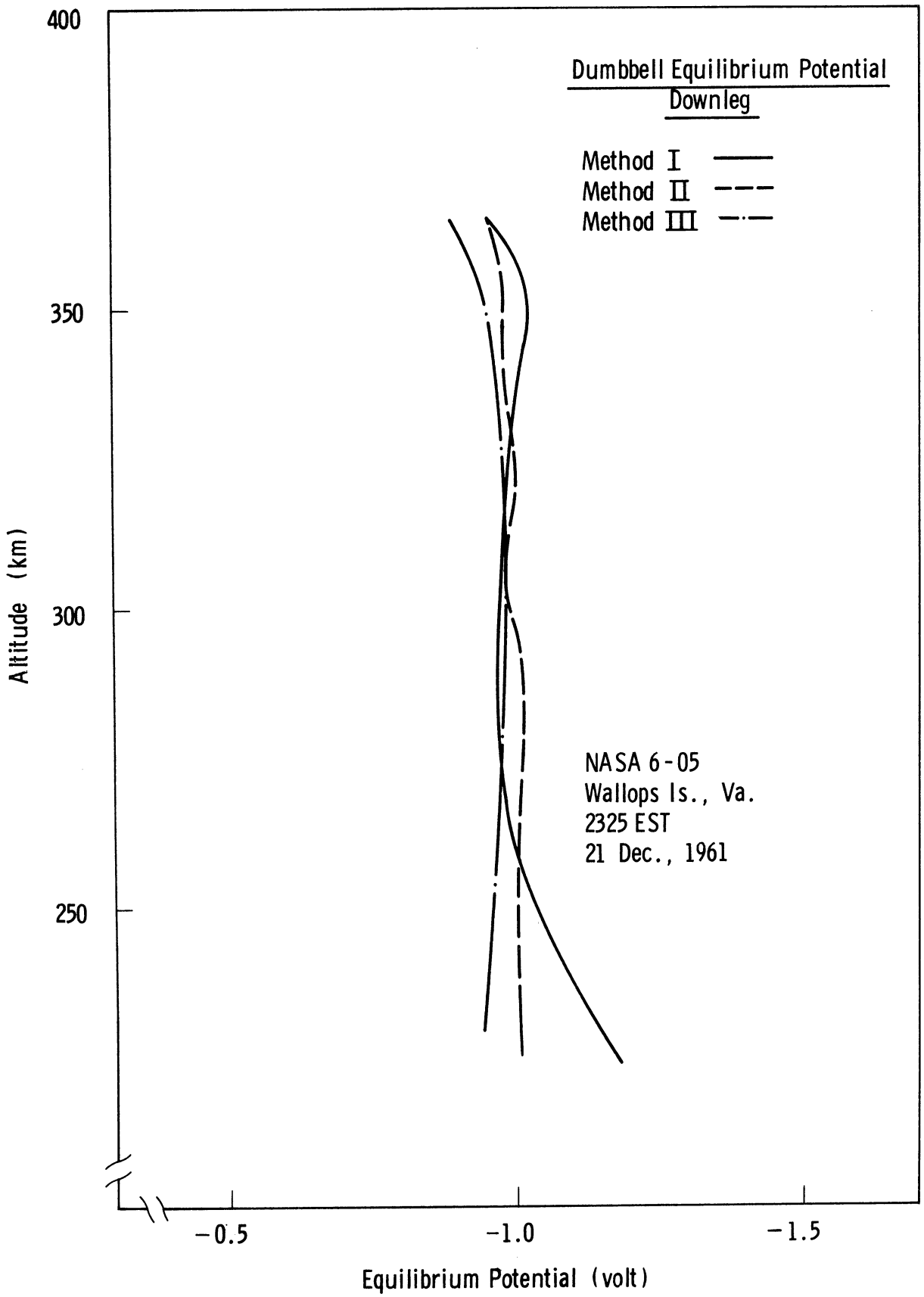

Fig. 7. Downleg Dumbbell equilibrium potential profiles obtained by the three methods.

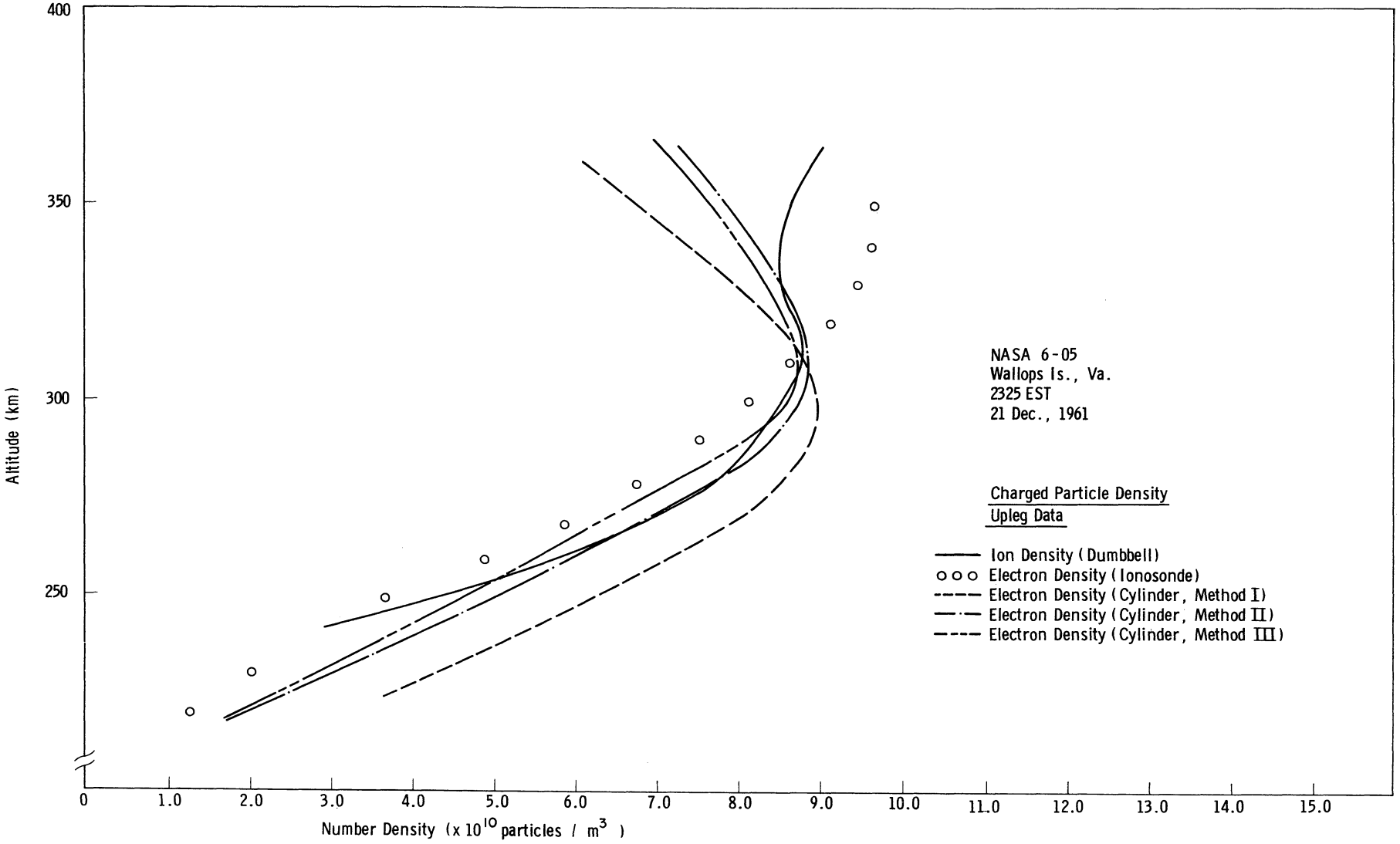

Fig. 8. Upleg electron density profiles obtained by the three methods. The ion density results from the Dumbbell experiment and the ionosonde results are also shown for comparison.

from the actual volt-ampere characteristics. Six to eight points from each curve were read into the computer and substituted into Eq. (6), for the number density N_e.

$$N_e = \frac{I_a}{\left(\frac{k\,T_e}{2\pi m_e}\right)^{1/2} q\,A\left[\frac{2}{\pi^{1/2}}\,V_o^{1/2} + \exp(V_o)\ \operatorname{erfc}(V_o^{1/2})\right]} \tag{6}$$

This equation is obtained from simple rearrangement of Eq. (4). Since N_e is assumed constant during one sweep, a value for the Dumbbell equilibrium potential, V_D, is obtained corresponding to each pair of data points. In this program a value of V_D is first calculated for all the possible combinations of pairs and from these an average value of V_D is obtained. This average value of V_D is then used to calculate the ambient electron density from each of the data points with the aid of Eq. (6). The resulting density values are then also averaged. These averaging processes minimize the reading errors, which can be considerable. The results of these calculations are shown in Figs. 6 to 9 (the V_D values are corrected as described on page 22.)

Another method, which is a variation of the one previously described (No. II), was also used to obtain electron density and Dumbbell potential information. This approach is again based on solving the accelerated electron current equation for V_D and N_e. Considering two points on the "accelerated" portion of the volt-ampere curves, the ratio of currents is

$$\frac{I_{a1}}{I_{a2}} = \frac{\frac{2}{\pi^{1/2}}(V_{o1})^{1/2} + \exp(V_{o1})\operatorname{erfc}(V_{o1})}{\frac{2}{\pi^{1/2}}(V_{o2})^{1/2} + \exp(V_{o2})\operatorname{erfc}(V_{o2})} = \frac{F(V_{o1})}{F(V_{o2})} \tag{7}$$

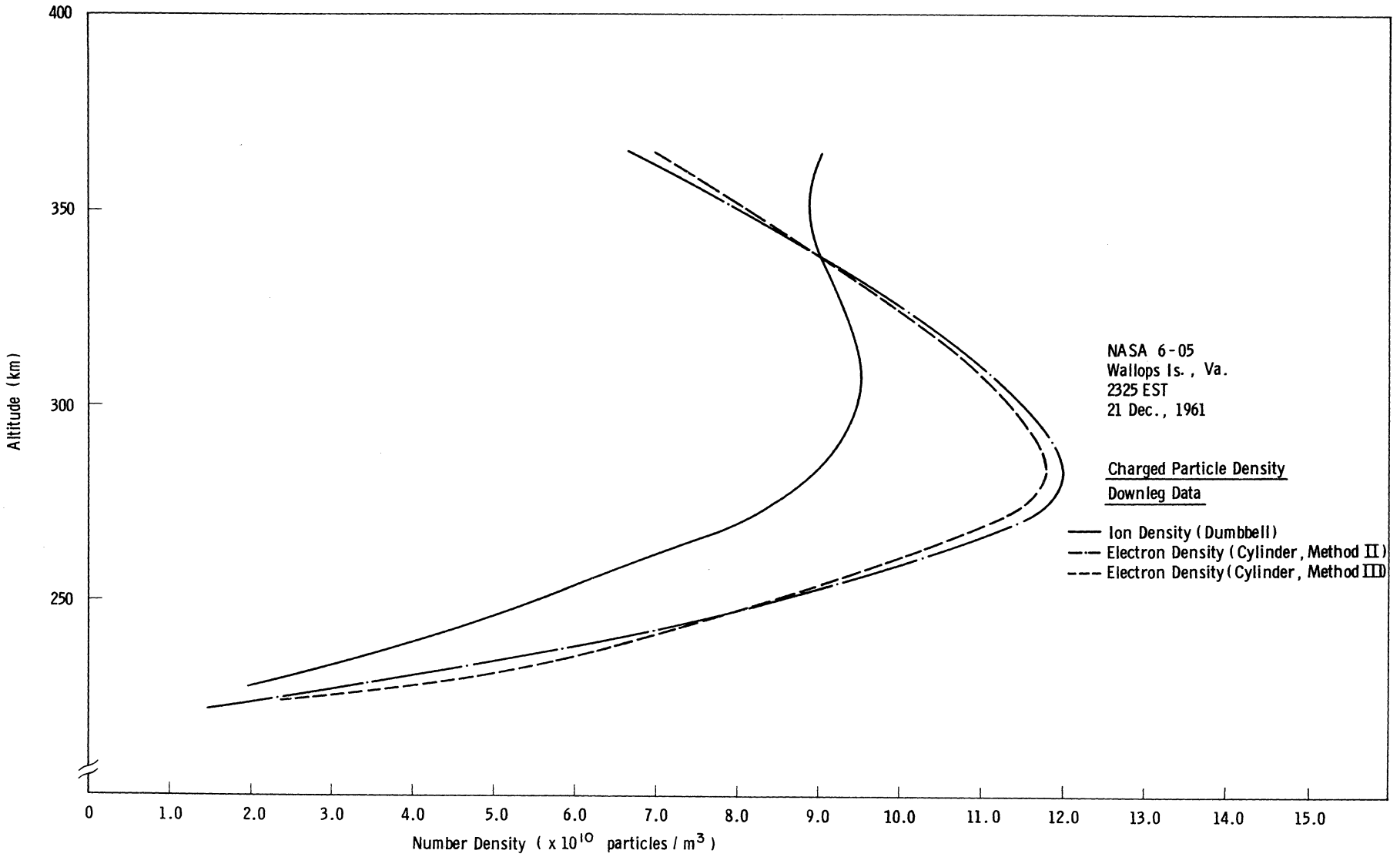

Fig. 9. Downleg electron density profiles obtained by Methods II and III and the ion density results from the Dumbbell experiment.

where $V_{on} = \frac{q}{kT_e} (V_{apn} + V_D)$, $n = 1,2...$

If the two points under consideration correspond to the maximum applied voltage, V_{apm}, and that applied voltage which brings the cylinder to the plasma potential, $|V_D|$, respectively, one can write:

$$\frac{I_{am}}{I_{er}} = F(V_{om}). \tag{8}$$

Equation (8) provides a functional relationship between I_{er} and V_D with V_{apm} as a parameter, thus:

$$I_{er} = G(V_D) \tag{9}$$

The experimental volt-ampere curve can be expressed as

$$I_k = H(V_k) \tag{10}$$

When $V_k = -V_D$, the measured current corresponds to the random current I_{er}. Thus if Eq. (9) is plotted on the same scale as the experimental curve the two curves will intersect at one point only. At this intersection point the applied voltage is equal in magnitude and opposite in sign to V_D and the current is the random current I_{er} from which the electron density can be computed [Eq. (5)]. In these computations, as previously, a small correction factor was applied to V_D (see p. 22) and the electron temperature values obtained from the Dumbbell mode of operation were used. A computer program was also written for this technique, which will be referred to as Method III, and the results are

shown in Figs. 6-9.

DISCUSSION

In predicting the characteristics of a bipolar probe it is convenient to plot the current to the individual electrodes in the fashion indicated in Fig. 10(c). The volt-ampere characteristics of a two-electrode combination can be determined from an inverted plot as shown in Fig. 10(c) by reading the voltage between the two curves for given current values. The necessary requirement of zero net current to the whole bipolar probe is inherently satisfied by a theoretical volt-ampere curve constructed in this fashion.

Such a curve (Fig. 11) was plotted using parameters typical of ambient conditions encountered during that portion of the flight from which the data were reduced. In constructing the characteristic curves of the Dumbbell the equations for a moving spherical body were used (Kanal, 1962). The theoretical curve indicates a Dumbbell equilibrium potential of about -0.5 volt as compared with about -1 volt determined from the experimental curves (e.g., Fig. 5). The reason for this difference is not understood at the present. It is believed to be due to any of the following effects or combinations thereof:

a. inadequacy of the equations used to describe the actual conditions;

b. difference in the work function of the electrodes (Medicus, 1961);

c. effective rectification of the radiated telemetry signal; and

d. charge buildup.

There is some experimental evidence of the last two named effects. On one of

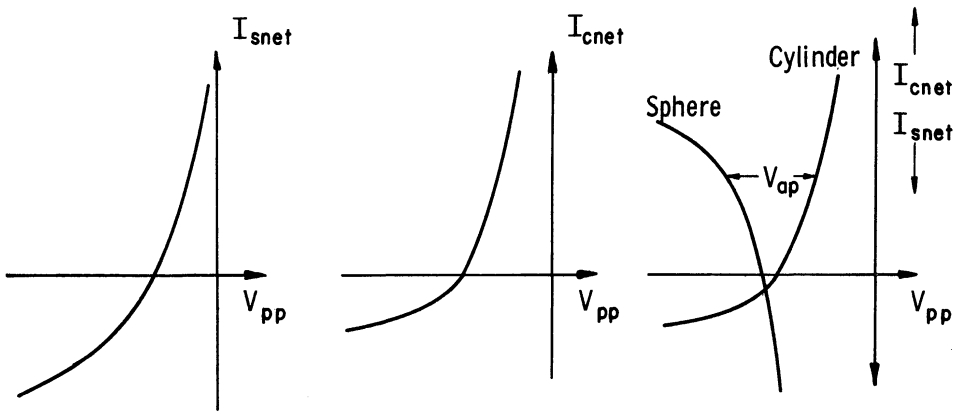

Volt-ampere characteristics of a single spherical probe (a)

Volt-ampere characteristics of a single cylindrical probe (b)

Combined volt-ampere characteristics of a sphere-cylinder bipolar probe (Note inverted sphere characteristics) (c)

Fig. 10. Theoretical volt-ampere characteristics of various probes.

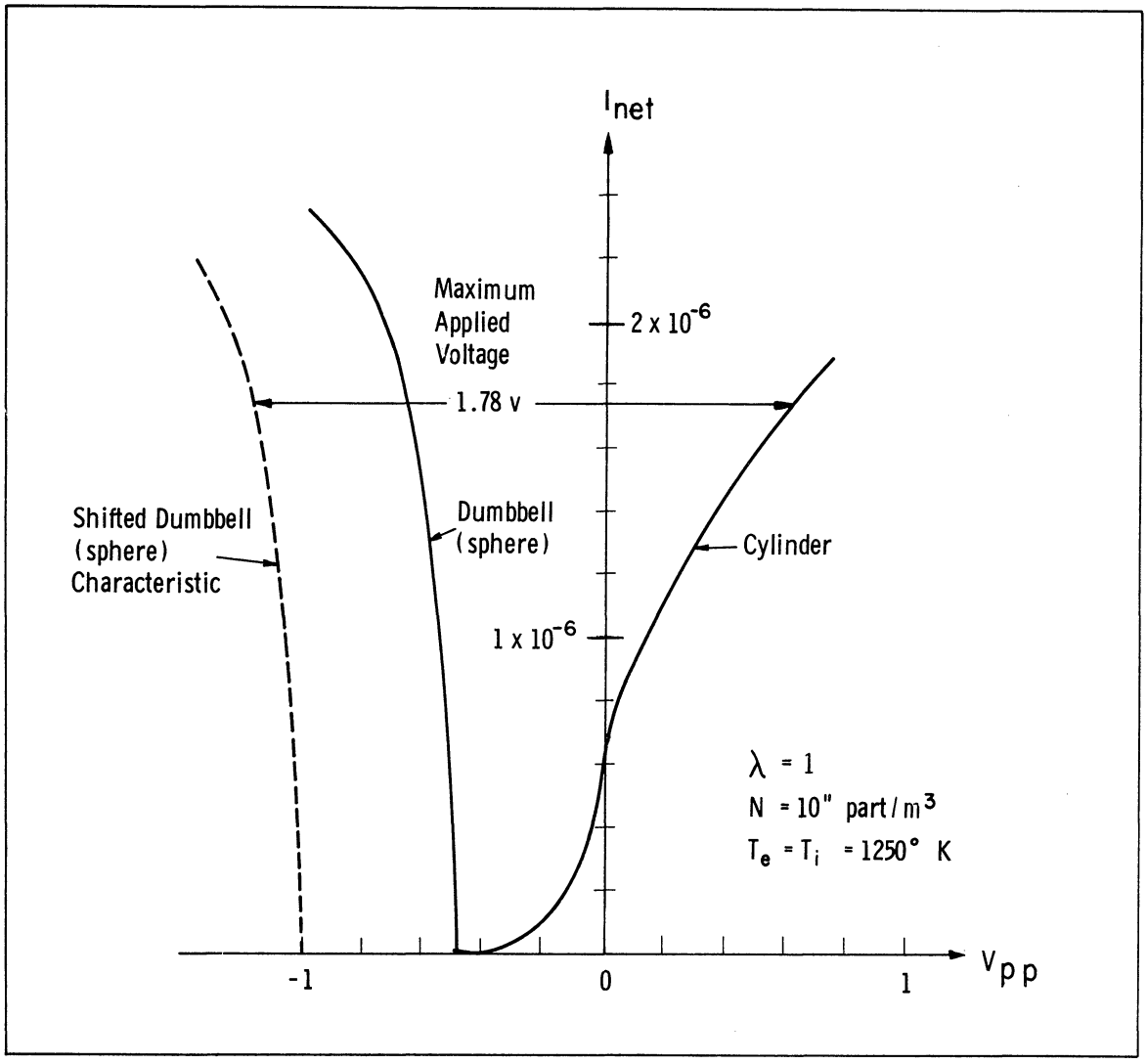

Fig. 11. Theoretical volt-ampere characteristic of a cylindrical probe for conditions typical of flight NASA 6.05.

the Dumbbell flights (NASA 6.04) the power radiated by the telemetry transmitter was reduced periodically by a factor of four, resulting in an apparent decrease of the equilibrium potential. No quantitative study of the magnitude of this voltage shift has yet been carried out. As far as effect (d) is concerned an examination of the upleg and downleg equilibrium potential profiles (Figs. 5 and 6) indicates an apparent increase in the potential with time, which could be interpreted as a slow charge buildup. This buildup has also been observed on other more recent flights.*

The dashed line in Fig. 11 is the theoretical Dumbbell curve shifted by 0.5 volt which is believed to approximate the actual conditions. (Note that the current on the experimental curve shown in Fig. 4 is also approximately zero up to an applied voltage of about 0.5V.) This theoretical curve indicates that when the cylinder is driven to the plasma potential, the potential of the Dumbbell has changed by about 3%. At the maximum applied potential the change is less than 10%.

The "breakpoint method" of analysis uses that portion of the volt-ampere characteristics where the cylinder is just at the plasma potential. The "voltage division" at that point is only 3%, which was decided to be too small to warrant any corrections. In the other two methods, the curves were analyzed in the region where the voltage division varies between 3-10% resulting in an overestimate of V_D somewhere between these two extremes. The V_D values calculated by these two methods are averages and therefore it was decided that a 7% reduction in the calculated values would give a good estimate of the true value. A somewhat higher value than the mean between the extremes was selected because more points from the higher voltage end of the curves were used.

*L. H. Brace, private communication.

The scatter in the Dumbbell equilibrium potential data from all the three methods is about the same. As an example, all the points obtained from the upleg data by Method II along with the resulting profile curve are shown in Fig. 12. The root-mean-square deviation of the data points from this curve is less than .06 volt. There is excellent agreement among the downleg results obtained by the three methods. There is some spread among the upleg curves at the lower altitudes, but they tend to converge near apogee.

The densities calculated by the breakpoint method are not directly dependent on this voltage division effect and therefore need no correction. The sensitivity of the current detector was such that the deflection at the point where the cylinder reaches the plasma potential is small (about 10% of full scale). The reading errors, therefore, introduced a large scatter in the data points as is indicated in Fig. 13, which shows the calculated upleg density points. The root-mean-square deviation about the curve drawn through these points is 1.38×10^{10} particles/m^3. The scatter in the downleg data was so bad that no attempt was made to construct a profile.

The results of upleg and downleg density data by both Methods II and III (with the modified V_D) is shown in Figs. 8 and 9. The curves in these figures correspond to lines drawn through the scatter of data points. Since in the calculations the computer program already does a certain amount of averaging, the scatter is less. As a typical example, the data points for the downleg curve derived by Method II are shown in Fig. 14. The root-mean-square deviation of the individual points about the curve is 0.7×10^{10} particles/m^3. The ion density profiles derived from the Dumbbell data are also shown for comparison in Figs. 8 and 9. The electron density profile obtained by

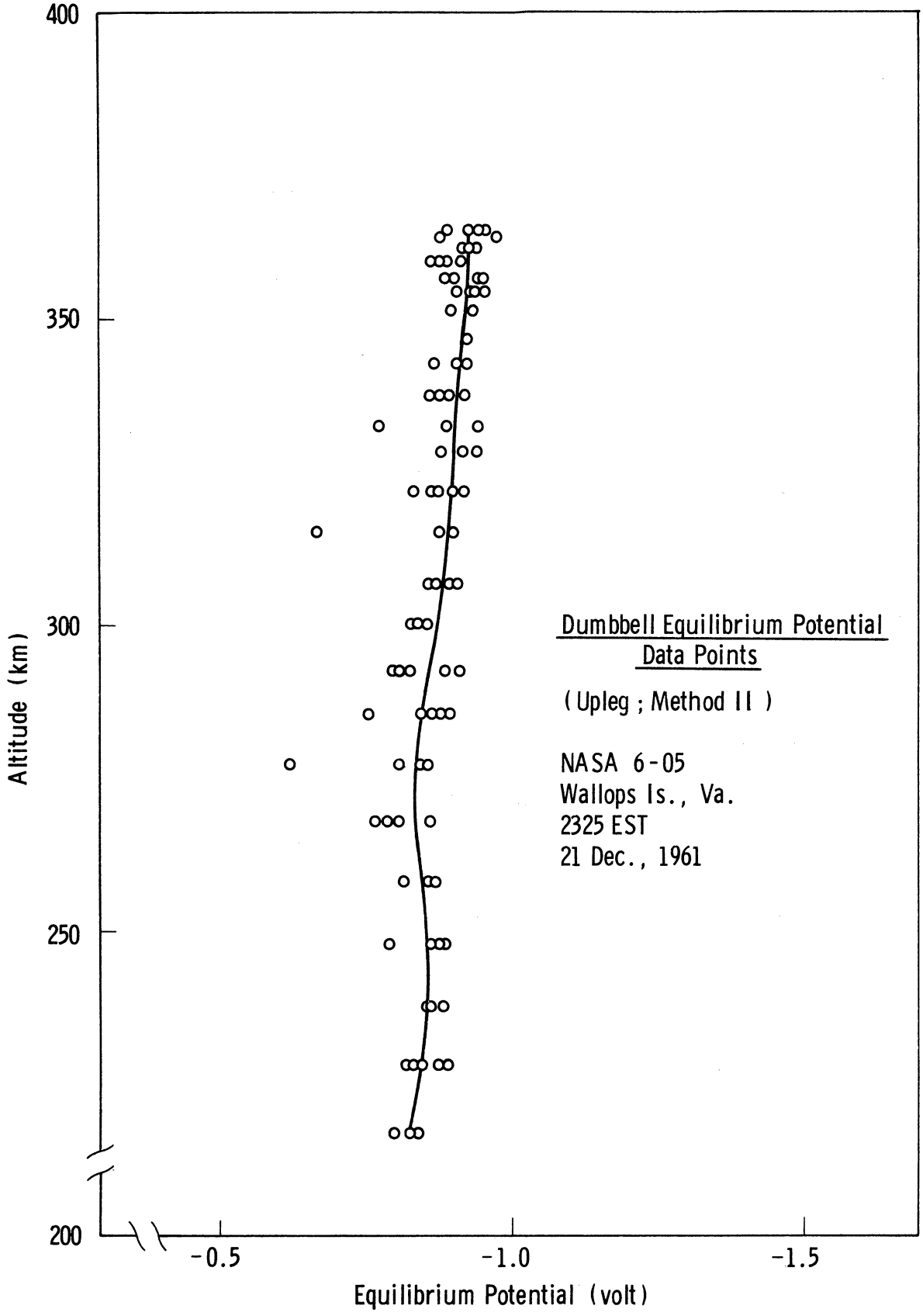

Fig. 12. Upleg Dumbbell equilibrium potential data points obtained by Method II. The profile corresponding to these points is also shown.

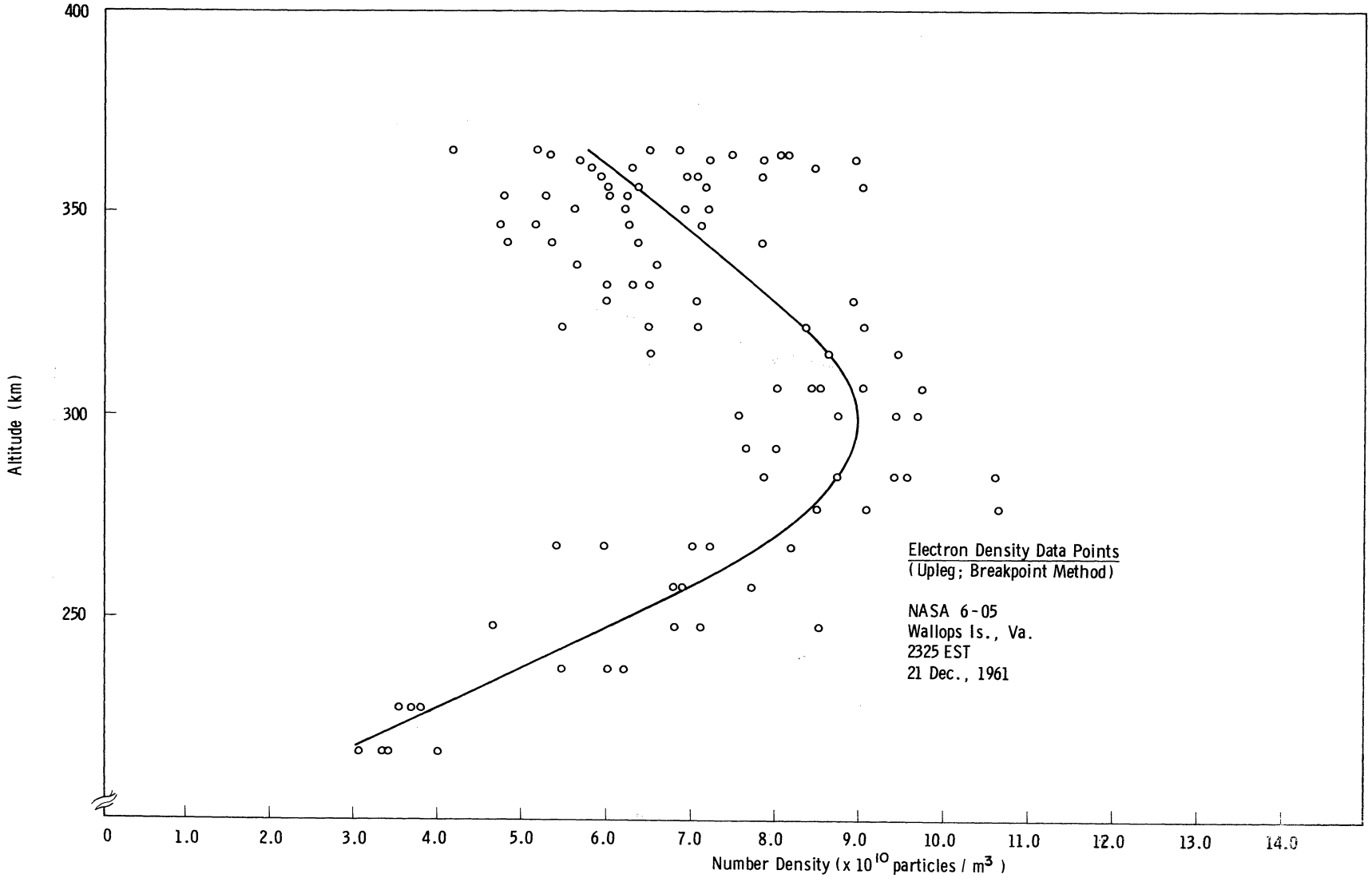

Fig. 13. Upleg electron density data points obtained by Method I. The profile corresponding to these points is also shown.

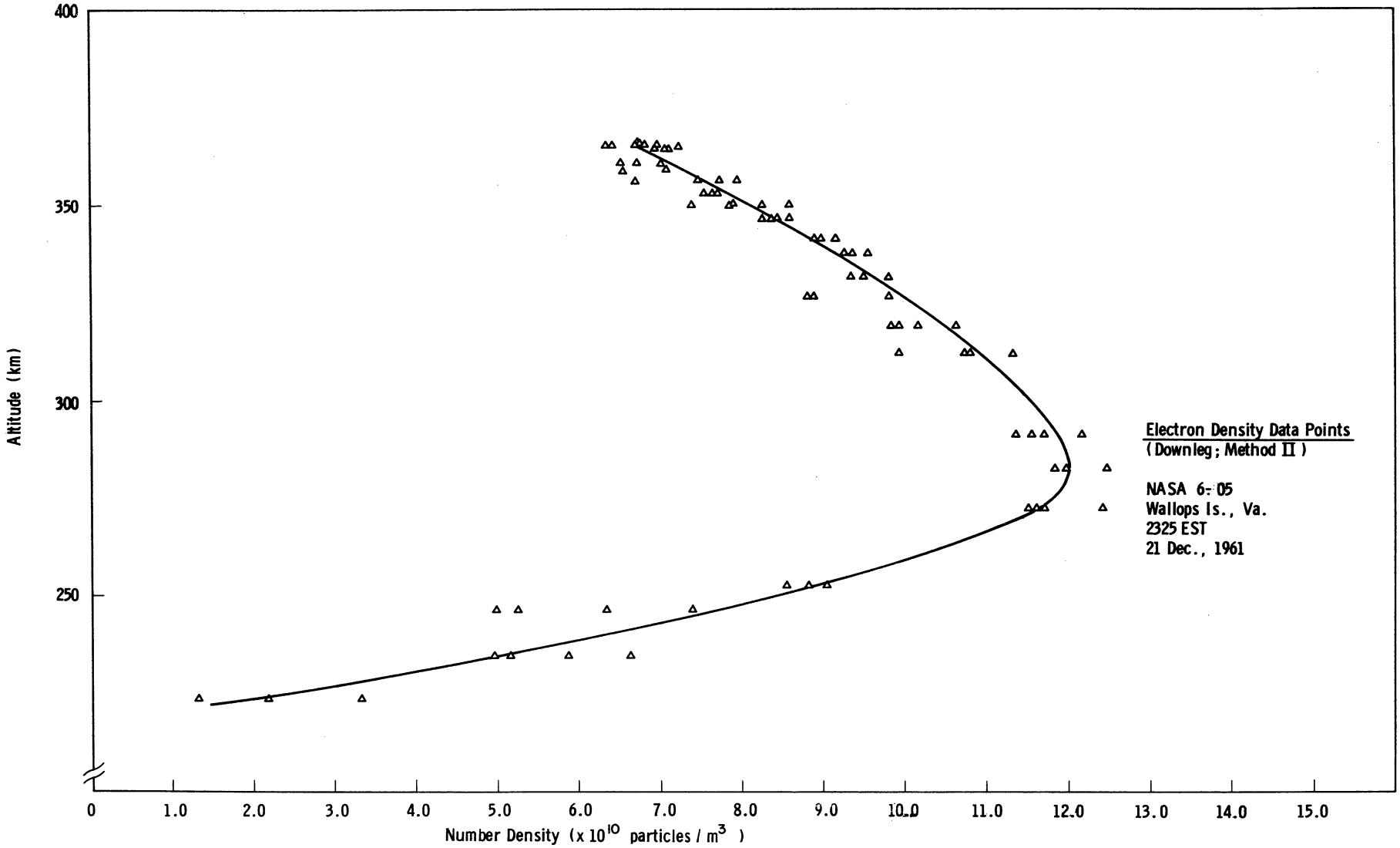

Fig. 14. Downleg electron density data points obtained by Method II. The profile corresponding to these points is also shown.

the ionosonde station at Wallops Island at launch time is shown with the upleg curves in Fig. 8. The agreement between the profiles obtained by Methods II and III and the major portion of the ion density curve is excellent. The agreement with the curve from Method I is not as good, but this is not surprising because of the resolution problems mentioned in the previous paragraph and the resulting spread in the data points. The deviation of the Dumbbell results, from those obtained by the other methods above about 330 km, is not significant, since it has been pointed out by Brace (1962) that the velocity dependent equations used to derive the ion density from the collected ion current have a tendency to overcorrect near apogee. The agreement among the peak densities measured by the ionosonde and the other methods is better than 10%. The altitude of the F_2 peak according to the ionosonde is at 347 km whereas the other measurements put this peak between 300-315 km. The cause of this disagreement may be due to the inherent difficulty of the ionosonde technique in assigning an actual height to the density peak, a condition aggravated at night when the unknown charge densities at lower altitudes become more significant (e.g., Rawer, 1957). Both the ion-and electron-density measurements indicate increased densities during the downleg portion of the flight; however, there is disagreement about the magnitude of this increase. The electron density values obtained from the cylinder by Methods II and III considerably exceed the ion density derived from the Dumbbell data (up to 25%). The altitude of the F_2 maximum on the downleg curves is between 285-305 km, which is a definite change from the upleg conditions. The high altitude of the F_2 peak measured by the ionosonde at the time of launch does follow this trend of decreasing altitude for the F_2 maximum. There was an approximately 20-minute local time change and a

3° latitude change between the beginning of the upleg and the end of the downleg portion of the flight, but these factors do not seem to be sufficient to explain these large changes. It should also be mentioned that the electron temperatures measured during the downleg portion of the flight differed by as much as 250°K from the upleg temperatures (Brace, 1962), indicating that the measurements were probably made during variable, somewhat anomalous, conditions.

This detailed study of the experimentally obtained volt-ampere characteristics has shown the feasibility of using such probes for ionospheric electron density measurements. The overall accuracy of such measurements can undoubtedly be improved from these reported here (estimated at about 15%) by optimizing the experiment parameters for density measurement. An even larger area ratio, a faster sweep, and greater applied voltage are but three of several changes which would significantly improve the measurement.

This study has also shown that the equilibrium potential of a reference body in the ionosphere can be determined by the analysis of the volt-ampere characteristics of a small cylindrical probe. The determination of this potential for the curves herein analyzed is believed accurate to better than 10%, which, as in the case of density determination, can be improved by proper choice of experimental parameters.

The data gathered by numerous recent cylindrical probe experiments are being processed and reduced by L. H. Brace of NASA's Goddard Space Flight Center. It seems certain that the accuracy of those experiments will be considerably better since the technique is being continually improved. This technique is rapidly reaching the point where it can be used to obtain accurate electron density infor-

mation, thus providing a new tool for direct measurements of the earth's ionosphere.

REFERENCES

Brace, L. H. "The Dumbbell Electrostatic Ionosphere Probe: Ionosphere Data." U of Mich. ORA Report 3599-11-F, September, 1962.

Brace, L. H., Spencer, N. W., and Carignan, G. R. "Ionosphere Electron Temperature Measurements and Their Implications." J. Geophys. Res., 68, 5397-5412, 1963.

Kanal, M. "Theory of Current Collection of Moving Cylindrical Probes." J. Appl. Phys., 35, 1697-1703, 1964.

Kanal, M. "Theory of Current Collection of Moving Sphericol Probes." U of Mich. ORA Report 03599-9-S, April 1962.

Medicus, G. "Theory of Probes with Non-Uniform Work Functions." Proceedings of the Fifth International Conference on Ionization Phenomena in Gases (ed. H. Maecker), pp. 1397-1405, North Holland Publishing Co., 1962.

Mott-Smith, H. M. and Langmuir, I. "The Theory of Collectors in Gaseous Discharges." Phys. Rev., 28, 727-763, 1926.

Rawer, K. "The Ionosphere." Frederick Ungar Publishing Co., New York, 1957.

Spencer, N. W., Brace, L. H. and Carignan, G. R. "Electron Temperature Evidence for Nonthermal Equilibrium in the Ionosphere." J. Geophys. Res., 67, 157-175, 1962.